



## EVALUATION OF THE SEISMIC BEHAVIOR FACTOR AND INTER-STORY DRIFT INDEX FOR CONFINED MASONRY BUILDINGS

E. Espinosa-Cazarin<sup>(1)</sup>, A. Terán-Gilmore<sup>(2)</sup>

<sup>(1)</sup> Doctoral student, Universidad Autónoma Metropolitana-Azcapotzalco, al2171800189@azc.uam.mx

<sup>(2)</sup> Professor, Universidad Autónoma Metropolitana-Azcapotzalco, tga@azc.uam.mx

### **Abstract**

The current version of the *Technical Complementary Requirements* (NTC, by its initials in Spanish) of the Mexico City Building Code (MCBC) was released on December 15, 2017. The NTC present several changes with respect to its previous version. Two of the most important ones was an increase in the maximum inter-story drift index allowed for the seismic design of confined masonry shear walls with horizontal reinforcement (the limit was doubled from 0.5% to 1%), and a reduction of the value of the seismic behavior factor (denoted  $Q$ ) for the design of confined masonry buildings taller than six stories

This paper offers a discussion on the pertinence of the maximum inter-story drift index considered by the current version of the NTC. Experimental data is presented, and the shortcomings of using the current allowable value for the inter-story drift index, for the seismic design of multi-story confined masonry buildings that develop a soft-story when deformed laterally, is discussed. To understand the impact of doubling the limiting value of inter-story drift index, several confined masonry buildings with varying number of stories were designed with the current version of the NTC. A series of static and dynamic nonlinear analyses were carried out to establish the structural properties and lateral response of the buildings. Based on that, a discussion is offered regarding the pertinence of the values of allowable inter-story drift index and seismic behavior factor currently under consideration by the MCBC.

*Keywords: Confined masonry buildings, Mexico City Buildings Code, Inter-story drift index, Seismic Behavior Factor*



## 1. Introduction

On December 15, 2017, the current version of the *Technical Complementary Requirements* (NTC) of the Mexico City Building Code (MCBC) was released. This document has several changes compared with the previous (2004) version. Two very important changes are related to the seismic design of confined masonry buildings. The first change doubled the inter-story drift index (*IDI*) allowed for horizontally reinforced confined masonry (from 0.5 to 1%), and the second one reduced the seismic behavior factor (*Q*) used for the design of buildings with more than six stories. Within the context of use of the NTC, *Q* can be understood as the maximum ductility demand allowed in the structural system, in such a manner that a  $Q = 1$  implies elastic behavior.

Both changes were justified with results obtained in recent experimental studies developed in the Mexican National Center on Disaster Prevention (CENAPRED, by its initials in Spanish) and the Engineering Institute of the National Autonomous University of Mexico (IINGEN-UNAM, by its initials in Spanish).

## 2. Experimental and Analytical Studies

### 2.1 Inter-story drift index

In 2015, Cruz Olayo. [1] carried out quasi-static experimental studies on the cyclic behavior of six confined masonry shear walls built with multi-perforated concrete units, and having different amount of horizontal reinforcement in the mortar joints.

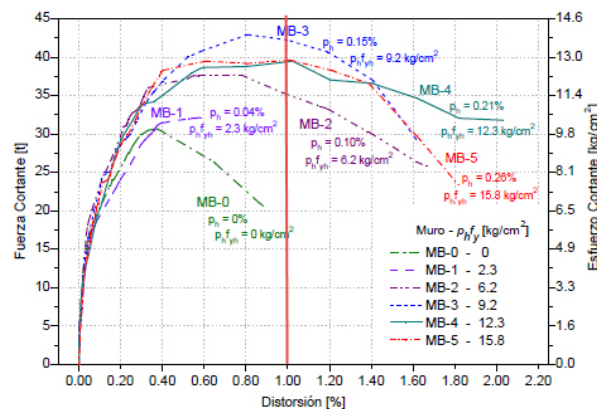


Fig. 1 – Back-bone curves corresponding to walls tested by Cruz-Olayo

According to Fig. 1, walls with horizontal reinforcement of at least  $6.2 \text{ kg/cm}^2$  ( $\rho_h f_{yh} \geq 0.60 \text{ MPa}$ ) can develop a lateral deformation corresponding to an *IDI* of 1%.

To evaluate the *dynamic effects* in the deformation capacity of confined masonry shear wall buildings with horizontal reinforcement, Flores *et al* [2] carried out in 2016 shaking table testing of a small-scale three-story masonry building (denoted M3ND-1). All walls had horizontal reinforcement of  $\rho_h f_{yh} = 0.65 \text{ MPa}$  (which can be considered representative of current Mexican practice). The strength of the model was primarily provided by two squat walls parallel to the direction of the seismic input, in such a manner that the total lateral strength of the model can be considered equal to the sum of the in-plane strength of both walls at the ground level. The model was subjected to a synthetic accelerogram that represented the maximum seismic demands the model can undergo if it was built in Mexico City.

Some of the preliminary conclusions proposed by the authors were: a) The failure mode of the walls was related to diagonal cracking in the wall panels and the fracture of the horizontal reinforcement; and b) The *IDI* accommodated by the model when its lateral strength was reduced to 80% of its maximum strength was equal to 1.7%

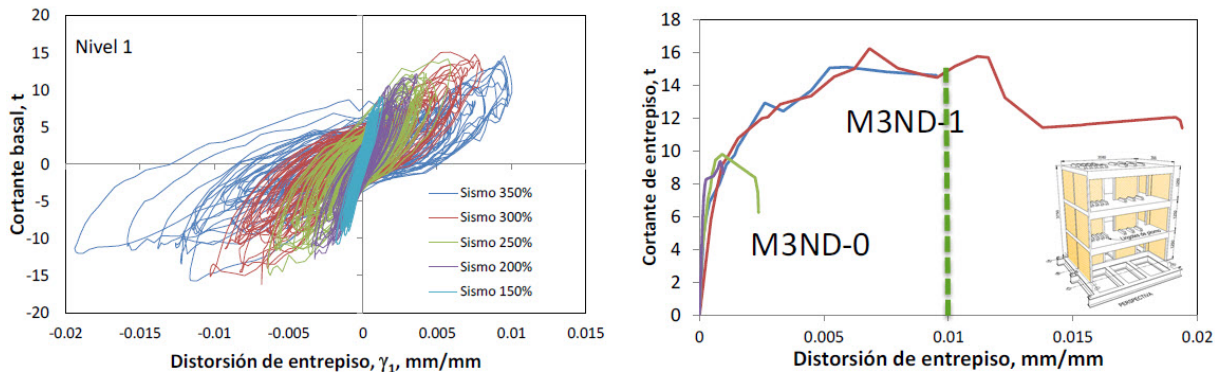


Fig. 2 – Cyclic response of M3ND-1 model: a) Hysteretic behavior; b) Back-bone curve

Fig. 2 shows the back-bone curve (*IDI* versus base shear) related to the ground story of the M3ND-1 model (where failure occurred). As can be seen, when the story reaches an *IDI* of 1%, the model keeps 93% of its maximum strength. The technical committee in charge of establishing the current version of the NTC noted that, the deformation capacity of confined masonry walls subjected to dynamic loading significantly increases with respect to that established from quasi-static testing. Particularly, it was observed that, according to Fig. 1, a squat confined masonry wall with horizontal reinforcement of  $0.60\text{MPa}$  could only accommodate, under quasi-static loading, an *IDI* of 0.5% when it develops its maximum shear strength; and that a similar wall studied under dynamic loading practically doubles, for that same condition, its *IDI*. Based on this, it was established, in a very approximate and empirical manner, that the *dynamic effect* modifies the deformation capability of confined masonry walls, and allows them to double the lateral deformation capacity established from quasi-static testing. This dynamic effect is mentioned and discussed in [3].

It should be mentioned that the *dynamic effect* due to seismic action will not necessarily double the lateral deformation capacity of every single confined masonry shear wall. Furthermore, an *IDI* of 1% does not represent the deformation capacity of confined masonry shear walls subjected to high compressive stresses. Particularly, once the lateral deformation of one such wall exceeds that associated with its maximum strength, the degradation of its structural properties has a significant dependence on the compressive axial load acting on it. On one hand, the larger the compression stress in the wall, the more unstable is its lateral behavior once the wall deforms beyond the deformation associated to its maximum lateral strength. This implies a more pronounced degradation of its hysteretic behavior, and a significant reduction in its lateral deformation capacity. On the other hand, the second-order effects ( $P-\Delta$ ) are increased. This results, as shown in Fig. 3a [4], in greater degradation of the lateral strength once the wall deforms beyond the deformation associated to its maximum strength. Since the stability of the wall at large lateral deformations depends on the combined effect of its hysteretic degradation and second-order effects, it is not pertinent to use the conclusions derived from the experimental response of walls subjected to low compressive stresses to anticipate the response of walls subjected to high compression stress. Therefore, care should be exercised when extrapolating the results derived from a very limited number of dynamic tests carried out in low-rise confined masonry buildings. To illustrate this, Fig 3b shows back-bone curves, established experimentally with quasi-static testing by Flores in 2019 [5], for masonry shear walls built with hollow clay units and subjected to different levels of compressive stress. The wall denoted MBRI-6 has twice the compression stress than the other ones. As a consequence, its lateral deformation capacity decreases with respect to that established for the walls with lower compressive stresses. It can be concluded first, that considering that the *dynamic effect* will double the deformation capacity of every single confined masonry wall is questionable at best, particularly for walls subjected to high compressive stresses; and second, that much more experimental testing under the consideration of dynamic loading should be carried out before fully understanding and quantifying the actual deformation capacity of confined masonry walls.

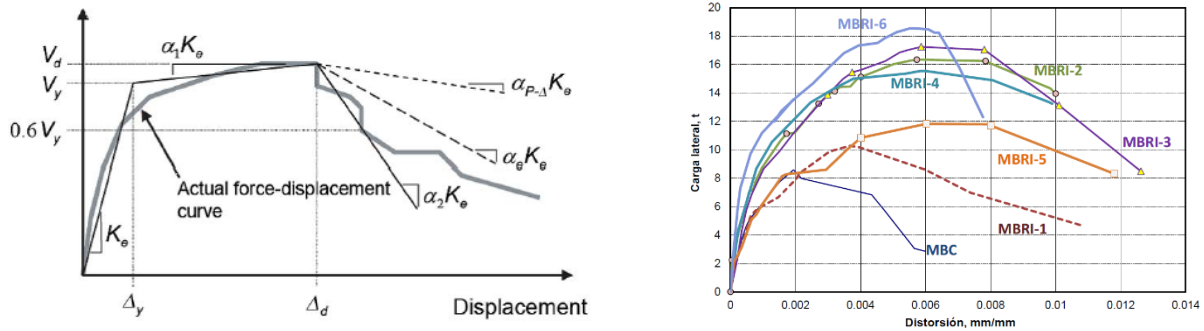


Fig. 3 – Axial compression load effect in the deformation capacity of walls: a) Combined effects of material degradation and second-order effects [4]; b) Confined masonry walls fabricated with hollow clay units [5]

## 2.2 Seismic behavior factor for mid-rise confined masonry buildings

The interstory shear maximizes in the ground story of masonry structures whose dynamic response is dominated by their fundamental mode of vibration. For masonry buildings with architectural plan (distribution of walls) constant along height, and under the assumption that in each story the walls have the same (or similar) lateral strength, the ground floor usually becomes, in relative terms, the weakest story. This is qualitatively shown in Fig. 4. Pérez Gavilan [3] proposes, for this type of systems, a simple model, originally developed by Paulay and Priestley, to estimate the maximum ductility demand on the ground floor ( $\mu_1$ ) as a function of the numbers of stories ( $n$ ) and the global ductility demand ( $\mu$ ):

$$\mu_1 = 1 + (\mu - 1)n\alpha \quad (1)$$

where  $\alpha$  is the effective mass factor. For the case of a masonry building with the same inter-story height and mass in all the stories:

$$\alpha = \frac{2n + 1}{3n} \quad (2)$$

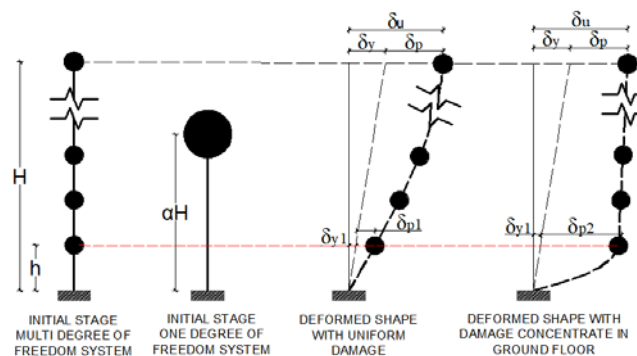


Fig. 4 –Variation of the elastic and inelastic displacement in a structure with uniform damage and damage concentrated on the ground floor.

Based on the experimental evidence of the deformation capacity of confined masonry squat shear walls with horizontal reinforcement and subjected to a compression stress equal to  $0.49\text{MPa}$ , tested under cyclic lateral load, Pérez Gavilán used an elasto-plastic idealization of their capacity curves and Equations 1 and 2 to establish that for the case of confined masonry, it is possible to design buildings up to 11 stories under the consideration of a global ductility of 1.5, and up to 7 stories for a global ductility of 2.0. This considerations were taken into account by the technical committees in charge of elaborating the current version of the NTC to establish a criterion that indicates that for confined masonry buildings with more than six stories, the seismic



behavior factor must be reduced in 0.5. This implies that for a horizontally reinforced confined masonry building with more than six stories, a  $Q$  of 1.5 must be used for its seismic design (instead of a value of 2.0 usually considered for low-rise buildings).

### 3. Buildings under consideration

To have an initial understanding of the impact of using the current NTC on the structural safety of mid-rise confined masonry buildings (CMBs), four CMBs were designed. Multi-perforated concrete  $120 \times 200 \times 400 \text{ mm}$  (IBMEX BH9) units with horizontal reinforcement were used. Residential use was considered for 8 and 10-story buildings. The analysis models of the buildings are shown in Fig 5. Two structural plans (Sirio and Agricola), inspired by those compiled by Cardel [6], were considered. All buildings are considered to have structural type II according to the NTC for the Design and Construction of Masonry Buildings (NTC-M), and to belong to Group B2 according to the NTC for Seismic Design (NTC-S).

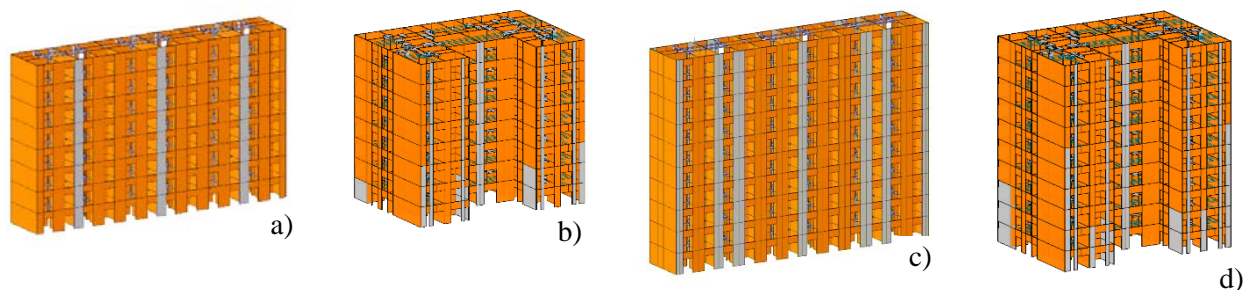


Fig. 5 – Structural analysis models for the four buildings: a) 8-story building with Sirio plan; b) 8-story building with Agricola plan; c) 10-story building with Sirio plan; d) 10-story building with Agricola plan

The irregularity and seismic behavior factors were established for each building according to the NTC-S. All buildings were assumed to be located in the Hill Zone of Mexico City. Because all buildings have more than six stories, their design spectra were established for  $Q$  of 1.5. A detailed review of the analysis and design of the buildings can be found in [7]

## 4. Nonlinear Static Analyses

### 4.1 Capacity curves and ultimate inter-story drift index

To estimate the structural properties of the buildings, capacity curves were established through a series of nonlinear static analyses, in both their principal directions. The lateral load pattern used for this purpose was proportional to the first mode of vibration. According to the discussion offered in [7], the nonlinear behavior of the confined masonry walls was considered through the modified wide-column model [8]. The nonlinear behavior of the walls considered their shear behavior, and was modeled with a trilinear back-bone curve. This back-bone model was recently proposed by the authors, and was calibrated with results derived from recent experimental testing of confined masonry walls [7]. It should be mentioned that the relative bending strength of all walls in the four buildings is considerably larger than their shear strength. As a consequence of this fact, which results from the design procedure contemplated by the NTC-M, the nonlinear model of the buildings does not have to contemplate explicitly the nonlinear bending behavior of the walls. The elastic shear stiffness was established by considering the height of the wall ( $H$ ), defined by the interstory height, the shear modulus ( $G_m$ ), and the shear area of the transformed section that considers the contribution of the tie columns through a modular ratio ( $A_v$ ). The shear stiffness was reduced in 50% to account for the effect of cracking [9]. The elastic bending stiffness was established by considering the boundary conditions, the modulus of elasticity ( $E_m$ ), and the transformed moment of inertia that accounts for the contribution of the tie columns ( $I$ ). The bending stiffness was also reduced in 50% to account for cracking [9].

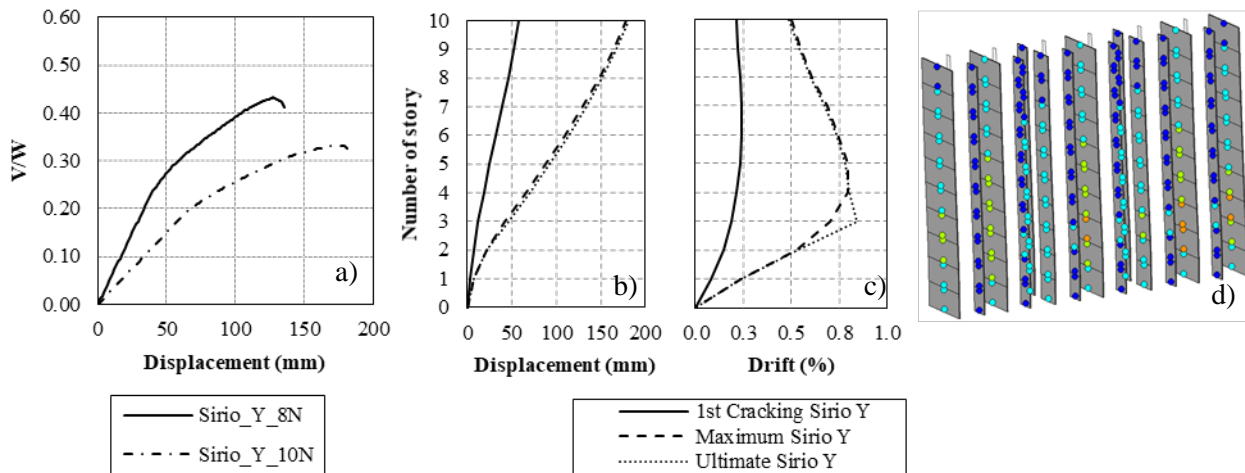


Fig. 6 – Static nonlinear analyses, transverse direction of Sirio plan buildings: a) Capacity curves; b) Displacement demands at different performance levels; c) Inter-story drift index at different performance levels; d) Hinge status at ultimate

While Fig. 6a shows the capacity curves for the transverse direction (Y direction) of buildings Sirio 8N and Sirio 10N, Figs. 6b and 6c show the distributions along height, for both buildings, of lateral displacement and *IDI* for the lateral deformation at which the first wall reached first cracking, maximum strength and ultimate deformation. It is possible to observe that, under a monotonic lateral deformation, not a single building is capable of developing an interstory drift index of 0.01 without developing a soft story.

One of the most important arguments offered by the committees in charge of updating the NTC-S and NTC-M to double the allowable *IDI* in confined masonry walls with horizontal reinforcement is the *dynamic effect*. To take into account this effect, the drifts related to maximum strength ( $IDI_{max}$ ) and ultimate deformation ( $IDI_{ult}$ ) of the walls was doubled with respect to those obtained with the back-bone curve discussed in [7] (calibrated from results obtained in quasi-static testing). New capacity curves were obtained under the consideration of the *dynamic effect*. Although as expected, the capacity curves that consider the *dynamic effect* indicate a larger deformation capacity, it does not avoid the development of soft stories in all buildings. Detailed results of all static nonlinear analyses are presented and discussed in [7]

#### 4.2 Estimation of seismic behavior factor

From the capacity curves, it is possible to estimate the ultimate ductility ( $\mu_u$ ) developed by the buildings, and based on it, the seismic behavior factor that should be used for their design. For this purpose, a bilinear idealization of each capacity curve was established by using the *equal-area method*. Once the roof displacement at yield was defined ( $\delta_y$ ), the ultimate global ductility can be estimated as a function of the ultimate roof displacement ( $\delta_u$ ):

$$\mu_u = \frac{\delta_u}{\delta_y} \quad (3)$$

The maximum ductility allowed for the seismic design of a structural system ( $\mu_{max}$ ) is established from the value of  $\mu_u$ . In the case of the NTC-S,  $\mu_{max}$  is about  $0.6\mu_u$  for a wide range of structural systems, and  $Q$  is considered to be equal to  $\mu_{max}$ , in such a manner that:

$$Q \approx 0.6\mu_u \quad (4)$$

Table 1 presents values of  $\mu_u$  established with the elasto-plastic idealization of the capacity curves (with and without considering the *dynamic effect*), and the values of  $Q$  established with Eq. 4. Even though for most of the cases contemplated in the table, a  $Q$  of 1.5 can be considered reasonable under the consideration of the *dynamic effect*, there are cases for which the actual value of  $Q$  is very close to its design value. If the *dynamic effect* is not considered, the design of 3 out of the 4 buildings yields unsafe structural systems. In every single



case, independently of the consideration or not of the *dynamic effect*, a soft story was developed at the ultimate roof displacement. Finally, a significant reduction in the value of  $Q$  can be observed for the Sirio and Agricola plans as the number of stories in the buildings increased from 8 to 10. For instance and under the consideration of the *dynamic effect*, the  $Q$  for the Sirio plan buildings decreases in the transverse direction from 2.37 to 1.54 as the number of stories go from 8 to 10. In the case of the Agricola plan buildings, this reduction goes from 2.51 to 1.8 in the transverse direction. The rate at which the value of  $Q$  decreases with an increase in the number of stories clearly indicates the danger, even under the consideration of the *dynamic effect*, of designing horizontally reinforced confined masonry buildings of more than 10 stories. If the *dynamic effect* is ignored, the design of the 8-story buildings under consideration herein must be considered unsafe.

Table 1 – Values of  $\mu$  established without and with the *dynamic effect* with an elastoplastic idealization

Building	Direction of analysis	Without <i>dynamic effect</i>					With <i>dynamic effect</i>				
		$\delta_y$	$V_y$	$\delta_u$	$\mu_u$	$Q$	$\delta_y$	$V_y$	$\delta_u$	$\mu_u$	$Q$
		(mm)	(kN)	(mm)			(mm)	(kN)	(mm)		
Sirio 8N	X	55	8770	219	3.98	2.39	65	9800	368	5.66	3.4
	Y	63	7400	135	2.14	1.28	70	8200	277.14	3.95	2.37
Agricola 8N	X	55	10900	148	2.69	1.61	51	11380	288	4.47	2.68
	Y	45	11190	116.76	2.59	1.55	45	12050	188.79	4.19	2.51
Sirio 10N	X	72	8570	267.90	3.72	2.23	82	9500	387.99	4.73	2.83
	Y	96	7265	181.22	1.88	1.13	105	7790	270.22	2.57	1.54
Agricola 10N	X	58	9800	191	3.29	1.97	62	10480	250.5	4.04	2.4
	Y	59	10290	129.61	2.19	1.31	64	11220	193.63	3.02	1.8

## 5. Nonlinear Dynamic Analyses

### 5.1 Calibration of the nonlinear model

To establish the maximum lateral deformation demands in the buildings, a series of nonlinear dynamics analyses were carried out. For this purpose, a hysteretic model was calibrated, as shown in Fig. 7, to reproduce the cyclic lateral behaviour of confined masonry shear walls. The experimental results shown in the figure were reported in [10]. A trilinear back-bone curve is considered for the hysteretic model. The first branch of the curve corresponds to elastic behaviour, before the lateral deformation of the wall reaches that associated with first cracking. The second branch corresponds to nonlinear behaviour with strain-hardening, and is delimited by the lateral deformations corresponding to first cracking and maximum strength. Finally, the third and final branch corresponds to lateral deformations exceeding that associated with the maximum strength in the wall, in which an increase in deformation results in a reduction of the strength of the wall before the wall reaches its ultimate deformation.

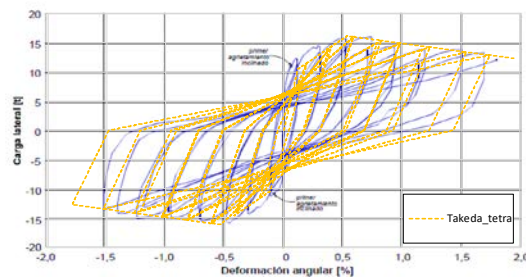


Fig. 7 – Calibration of the hysteretic model for confined masonry shear wall



## 5.2 Selection and scaling of the ground motions

A series of 8 ground motions were selected and scaled. Four motions were recorded during subduction earthquakes (*SU*), and the rest during intermediate depth (*ID*) earthquakes. All motions were recorded during actual events at the FJ74 accelerometric station. For each motion, a single pseudo-acceleration spectrum was established by geometrically adding the spectral ordinate of each component for 5% of critical damping. The ground motions were linearly scaled in such a manner that the average of the spectral ordinates for the 8 motions reasonably covered, in a range of periods going from 0.2 to 1.3 times the fundamental period of the structure, the ordinates of the design elastic spectrum multiplied by 1.3. Table 2 summarizes some properties of the motions and their corresponding scaling factors.

Table 2 –Motions used for the nonlinear dynamic analysis

Record	Date	PGA ( $cm/seg^2$ )		$M_w$	Duration ( $sec$ )	Scale Factor			
		N00E	N90W			Sirio		Agricola	
						8N	10N	8N	10N
<i>IDX1</i>	23/05/1994	6.35	8.10	5.6	85.39	15.2	26	20	20
<i>IDY1</i>	15/06/1999	21.84	18.43	6.9	175.75	7	8	6.5	6.3
<i>IDX2</i>	11/12/2011	26.39	26.47	6.5	202.75	6	8	10	10
<i>IDY2</i>	19/09/2017	93.32	90.95	7.1	226	1.8	2	1.6	1.6
<i>SUX1</i>	20/03/2012	11.29	16.35	7.5	234.75	10.5	12	12.2	12.2
<i>SUY1</i>	08/05/2014	18.97	13.68	6.4	216.6	9.5	12	10	10
<i>SUX2</i>	10/12/1994	5.36	4.95	6.4	85.24	23.5	29	26	26
<i>SUY2</i>	14/09/1995	10.46	9.71	7.3	138	14.4	14	14.5	14.5

Fig 8. shows in gray lines, for the Sirio 10N building, the pseudo-acceleration and displacement spectra for the 8 scaled ground motions. The black line represent the design spectra multiplied by a factor of 1.3. The red lines correspond to the average spectra for the 8 records. The vertical blue line corresponds to the fundamental period of the building ( $T$ ), and the green and purple lines delimit the period range going from 0.2 to 1.3 $T$ .

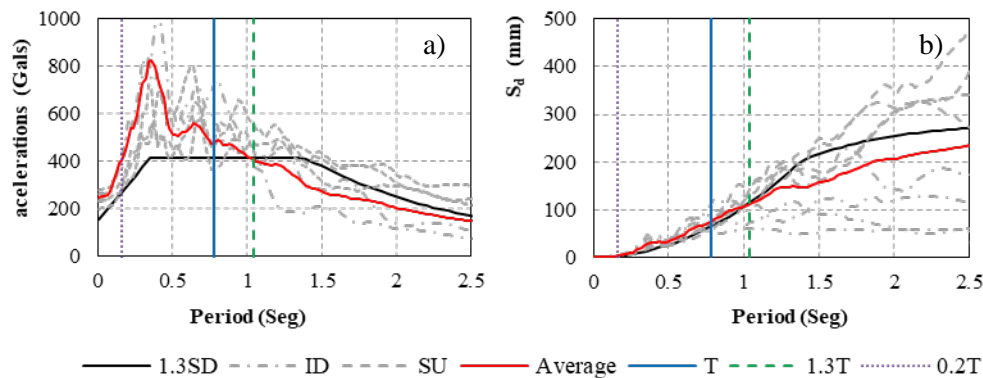


Fig. 8 – Spectra corresponding to scaled ground motions, Sirio 10N building: a) pseudo-acceleration; b) displacement

## 5.2 Seismic performance

A series of dynamic nonlinear analyses were carried out for all buildings under consideration. The results shown herein only consider the analytical models that neglect the *dynamic effect*. Fig. 9 shows the distribution of lateral deformation along height for the record *IDY1*. The maximum roof displacement ( $\delta_{roof}$ ) in the Sirio 10N building is 126mm, with a maximum *IDI* demand of 0.0054. Fig. 9c shows the hysteretic behavior of the wall that developed the largest nonlinear demand; and Fig. 9d shows the hinge status in all walls for the



maximum  $\delta_{roof}$  demand. A blue circle indicates that the wall is working within its elastic range of behavior, and a green circle that the wall has developed nonlinear behavior but has not reached the lateral deformation associated to its maximum strength (its behavior falls in the second branch of the trilinear back-bone curve).

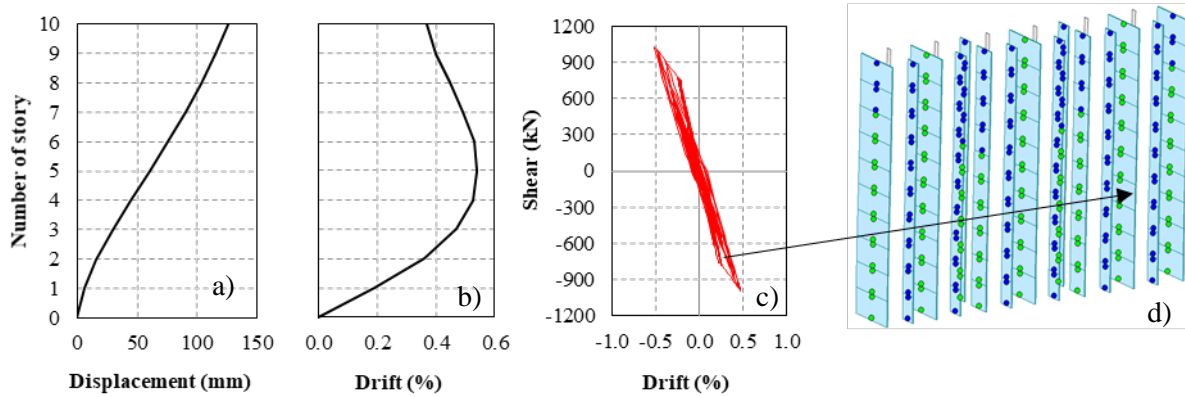


Fig. 9 – Distribution of lateral deformation along height, nonlinear dynamic analysis, *IDYI* record: a) Lateral displacement; b) Inter-story drift index; c) Hysteretic behavior of wall that developed largest nonlinear deformation; d) Hinge status at maximum roof lateral displacement

Based on the nonlinear demands obtained from the dynamic nonlinear analyses, it is possible to conclude that all buildings accomplish the design objectives established in the NTC-S, in the sense that the nonlinear demands have not gone beyond that associated to the maximum strength of the walls. Not a single wall developed an *IDI* of 0.01. The maximum global ductility developed by the building by considering  $\delta_y = 96\text{mm}$  (see Table 1, without *dynamic effect*) is equal to 1.31, which is smaller than the value of  $Q$  used during its design (1.5). If the *dynamic effect* is not considered in the dynamic nonlinear analyses, the lateral deformation demands in the walls are very close to the maximum allowed by the NTC-S, which corresponds to that in which the walls developed their maximum strength. It can be concluded that the design is barely adequate, and has little reserve capacity to accommodate an extraordinary earthquake event.

### 5.3 Incremental dynamic analysis

In the case of buildings with structural members that develop unstable nonlinear behaviour once their lateral deformation goes beyond that associated to its maximum strength, it is possible that they evolve, with a small increment in their lateral deformation, from a state of moderate damage to global instability. To study this possibility, it was decided to carry out an incremental dynamic analysis in the transverse direction of the Sirio 10N building by linearly scaling up the *IDYI* record.

Fig. 10 shows the distribution of lateral deformation along height corresponding to different scaling factors. The scale factors in the figure are applied simultaneously with those under consideration in Table 2 to scale the ground motions above the intensity level under consideration in the design spectra determined with the NTC-S. The smallest value under consideration for the scale factor in Fig. 10 (equal to 1.12) was established in such a manner that the wall with the largest nonlinear demands develop a lateral deformation equal to that associated to its maximum strength. Thus, scaling factors larger than that produce nonlinear demands that result in walls developing nonlinear demands that go beyond that associated to the maximum strength of the walls (the walls reach the third branch of the trilinear back-bone curve). For a scale factor of 1.12, the maximum  $\delta_{roof}$  is equal to 139mm and the maximum global ductility is equal to 1.44. As shown in Fig. 10c and indicated with the red circles in Fig. 10d, several walls located in the second and third stories have incipiently developed a negative slope. However, and according to the hysteretic behavior of the walls, their maximum deformation demand has not surpassed their ultimate deformation capacity.

In terms of the global dynamic instability of the Sirio 10N building, the building becomes unstable, as shown in Figure 11, once the scaling factor reaches values larger than 2.24 ( $\delta_{roof}$  is equal to 218mm and  $\mu$  equal to 2.27). Fig. 11b shows the hysteretic behaviour of the wall with the largest nonlinear demand for scaling factors



of 2 (black line) and 2.24 (red line), and Fig. 11c the hinge status corresponding to the maximum roof displacement for a scaling factor of 2.24. Global instability occurs just after the fourth story reaches an interstory drift index of 0.01. It can be concluded that structural failure in the transverse direction of the Sirio 10N building is likely to occur due to material degradation and failure rather than a global dynamic instability.

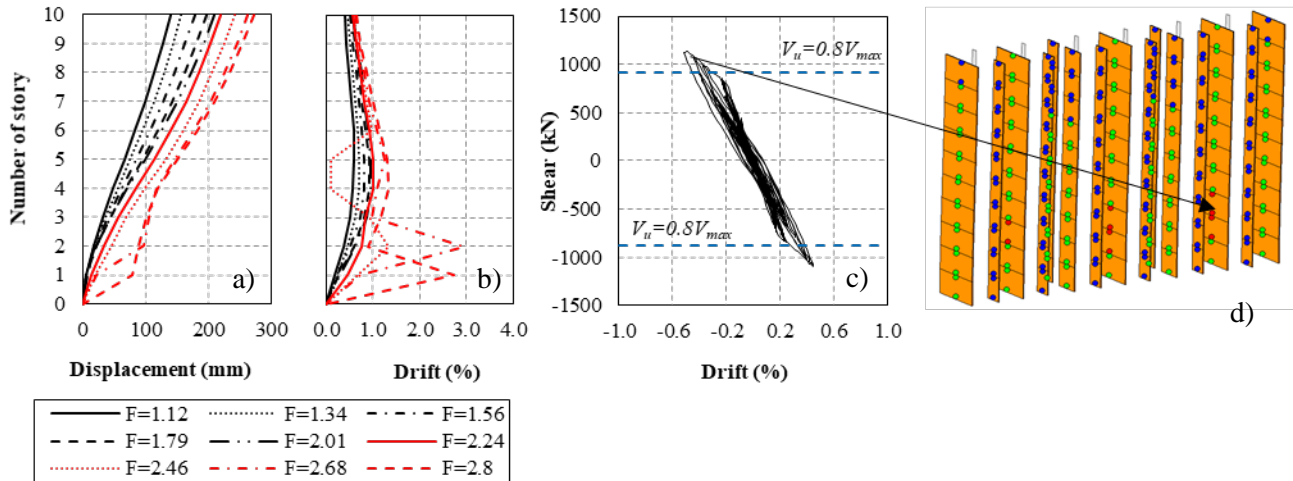


Fig. 10 – Distribution of lateral deformation along height, incremental nonlinear dynamic analysis, *IDYI* record: a) Lateral displacement; b) Inter-story drift index; c) Hysteretic behavior of wall that developed largest nonlinear deformation; d) Hinge status at maximum roof lateral displacement

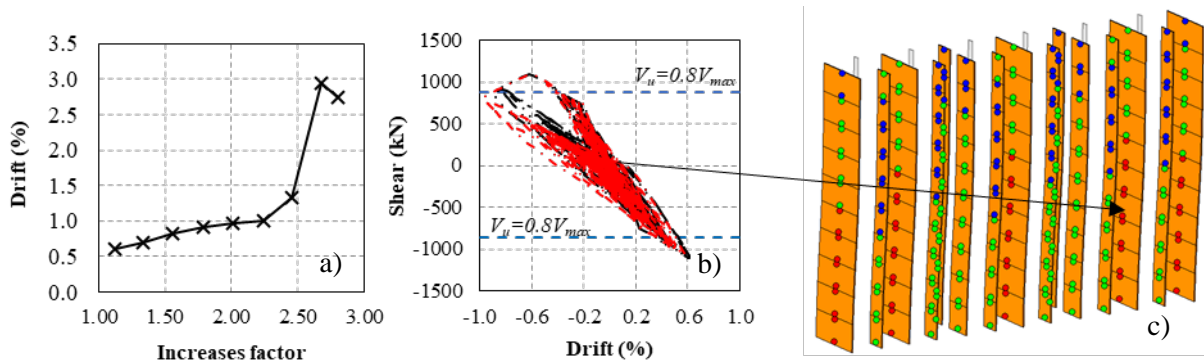


Fig. 11 – Study of dynamic instability, Sirio 10N building, *IDYI* record: a) Maximum inter-story drift index as a function of the scaling factor; b) Hysteretic behavior of wall with largest nonlinear demand, scaling factor of 2; c) Hinge status for maximum roof displacement, scaling factor of 2

## 6. Conclusions

A thorough discussion about the *IDI* and *Q* for the seismic design of mid-rise confined masonry buildings proposed in the current version of the NTC was offered. According to this, some of the evidence that justify this values may not be applicable for medium-rise confined masonry buildings. Four buildings were designed and their structural properties were established with a series of nonlinear static analysis. It was possible to observe, that regardless of whether the dynamic effect on the deformation capacity of the walls is considered or not, once a masonry building reaches its maximum strength, only a minimum increase in lateral displacement is necessary to reach a state of global instability. Based on the results of nonlinear static analyses, it is possible to conclude that a *Q* of 1.5 for the design of confined masonry buildings with horizontal reinforcement can result in insecure medium-rise building. To establish the maximum lateral deformation demands (displacements and drift) and the performance in the buildings, a series of nonlinear dynamics analyses were carried out. With the result obtained in the dynamic nonlinear analysis is possible to conclude that all buildings accomplish the



requirements established in the NTC-S. An incremental nonlinear dynamic shows that for a incremental factor of 2.24 the Sirio Building become unstable and a soft story is develop bewteen the second and third story with a  $IDI$  near to 0.01, a  $\delta_{roof}$  of 218mm and a  $\mu$  of 2.2. these values are bigger that those found in the nonlinear static analysis

Neither experimental nor analytical studies provide a solid enough basis for the inter-story drift limit value and the seismic behaviour factor considered by the NTC-S for the design of medium-rise confined masonry buildings with horizontal reinforcement in Mexico City. These values are too optimistic, and make it possible to design buildings that not meet the implicit safety requirements in the use of the NTC. In the short term, it is important to limit the number of floors allowed for masonry buildings built in Mexico City and; In long term, the development of design requirements that take into account the level of axial load and the aspect ratio of the masonry walls in determining the maximum inter-story drift index, and seismic design values used for the design.

## 7. Acknowledge

The authors wish to express their gratitude to Prof. Juan Jose Perez-Gavilan and S.E. Raul Jean for provid-ing information relevant to the study reported herein. The first author wishes to express his gratitude to the Mexican National Council of Science and Technology (CONACYT) for the scholarship received to carry out his doctoral studies.

## 8. References

- [1] Cruz-Olayo A. (2015). Contribucìon del refuerzo horizontal a la resistencia de muros de mampostería confinada. Msc Thesis, Universidad Nacional Autónoma de Mèxico (in spanish)
- [2] Flores L, Pèrez Gavilàn J, Duràn R. (2016). Ensaye de dos estructuras de mampostería confinada de tres niveles a escala 1:2, variando el refuerzo horizontal. *XX congreso nacional de ingeniería estructural, Merida, Yucatan, Mèxico* (in spanish)
- [3] Pérez Gavilàn J. (2019). Ductility of confined masonry walls; Results from several experimental campaigns in Mexico, *13<sup>th</sup> North American Masonry Conference, Salt Lake City, Utah, USA*
- [4] ASCE/SEI (2014). Seismic evaluation and retrofit of existing buildings (ASCE/SEI 41-13): American Society of Civil Engineers
- [5] Flores L, (2019). Ensaye de muros de bloque hueco de concreto con refuerzo interior cante carga lateral. *XXII Congreso Nacional de Ingeniería Sismica, Monterrey, Nuevo Leon, Mèxico* (In Spanish)
- [6] Cardel O. (2015) Estudio analítico de la interacción momento-cortante en muros de mampostería. Msc Thesis, Universidad Nacional Autonoma de Mèxico. (in spanish)
- [7] Espinosa-Cazarin E. Teràn-Gilmore A. (2020) Estabilidad global y capacidad de deformación de edificios de mediana altura de mampostería confinada diseñados con las normas técnicas complementarias de la Ciudad de Mèxico. *Revista internacional de ingeniería estructural (in press)* (in Spanish)
- [8] Terán-Gilmore A. Zuñiga-Cuevas O. Ruiz-Garcia J. (2009). Displacement-based seismic assessment of low-height confined masonry walls. *Earthquake Engineering & Structural Dynamics*, 26(10), 1059-1071. [oi:10.1002/\(SICI\)1096-9845\(199710\)26:10<1059::AID-EQE694>3.0.CO;2-M](https://doi.org/10.1002/(SICI)1096-9845(199710)26:10<1059::AID-EQE694>3.0.CO;2-M)
- [9] NIST (2014) Seismic design of special reinforced masonry shear walls: Aguide for practicing engineers. Gaithersburg MD.
- [10] Aguilar G. Alcocer S. (2001) Efecto del refuerzo horizontal en el comportamiento de muros de mampostería confinada ante cargas laterales. CENAPRED (in spanish)